Published OnlineFirst April 16, 2018; DOI: 10.1158/0008-5472.CAN-16-1701

Tumor Biology and Immunology

Cancer Research

Sustained Adrenergic Signaling Promotes Intratumoral Innervation through BDNF Induction

Julie K. Allen[1], Guillermo N. Armaiz-Pena[1], Archana S. Nagaraja[1], Nouara C. Sadaoui[1], Tatiana Ortiz[2], Robert Dood[1], Merve Ozcan[1,3], Danielle M. Herder[1], Monika Haemmerle[1], Kshipra M. Gharpure[1], Rajesha Rupaimoole[1], Rebecca A. Previs[1], Sherry Y. Wu[1], Sunila Pradeep[1], Xiaoyun Xu[4], Hee Dong Han[1], Behrouz Zand[1], Heather J. Dalton[1], Morgan Taylor[1], Wei Hu[1], Justin Bottsford-Miller[1], Myrthala Moreno-Smith[1], Yu Kang[1], Lingegowda S. Mangala[1], Cristian Rodriguez-Aguayo[5], Vasudha Sehgal[6], Erika L. Spaeth[7], Prahlad T. Ram[6], Stephen T.C. Wong[4,8], Frank C. Marini[9], Gabriel Lopez-Berestein[5,10], Steve W. Cole[11], Susan K. Lutgendorf[12,13,14], Mariella De Biasi[15], and Anil K. Sood[1,10,16]

Abstract

Mounting clinical and preclinical evidence supports a key role for sustained adrenergic signaling in the tumor microenvironment as a driver of tumor growth and progression. However, the mechanisms by which adrenergic neurotransmitters are delivered to the tumor microenvironment are not well understood. Here we present evidence for a feed-forward loop whereby adrenergic signaling leads to increased tumoral innervation. In response to catecholamines, tumor cells produced brain-derived neurotrophic factor (BDNF) in an ADRB3/cAMP/Epac/JNK-dependent manner. Elevated BDNF levels in the tumor microenvironment increased innervation by signaling through host neurotrophic receptor tyrosine kinase 2 receptors. In patients with cancer, high tumor nerve counts were significantly associated with increased BDNF and norepinephrine levels and decreased overall survival. Collectively, these data describe a novel pathway for tumor innervation, with resultant biological and clinical implications.

Significance: Sustained adrenergic signaling promotes tumor growth and metastasis through BDNF-mediated tumoral innervation. *Cancer Res; 78(12); 3233–42. ©2018 AACR.*

Introduction

There is increasing evidence that chronic sympathetic nervous system activation can lead to increased norepinephrine levels in the tumor microenvironment (1–3). However, the underlying mechanisms behind this observation have remained largely unknown. Increased norepinephrine in the tumor has been associated with the induction of growth promoting signals that are largely mediated by β-adrenergic receptors on tumor cells (4–7). For example, increased adrenergic signaling has been associated with increased tumor growth and progression that is fueled by activation of protumoral factors, such as STAT-3, IL6, VEGF, FAK, and Src (4, 8). Moreover, it has been shown that β-blockers can reduce or abrogate the effects of chronic restraint stress in animal models of disease (3, 4). Interestingly, although some studies have found tumoral innervation (1, 9), the underlying mechanism and downstream effects of this process are not well understood. Here, we investigated the mechanisms responsible for tumor-induced innervation, allowing catecholamine

[1]Department of Gynecologic Oncology and Reproductive Medicine, The University of Texas M.D. Anderson Cancer Center, Houston, Texas. [2]Division of Cancer Biology, Ponce Research Institute, Ponce, Puerto Rico. [3]Department of Basic Oncology, Hacettepe University Cancer Institute, Ankara, Turkey. [4]Systems Medicine and Bioengineering Department, Houston Methodist Research Institute, Weill Cornell Medical College, Houston, Texas. [5]Department of Experimental Therapeutics, The University of Texas M.D. Anderson Cancer Center, Houston, Texas [6]Department of System Biology, The University of Texas M.D. Anderson Cancer Center, Houston, Texas. [7]Department of Leukemia, The University of Texas M.D. Anderson Cancer Center, Houston, Texas. [8]Department of Pathology, Genomic Medicine and Radiology, Houston Methodist Hospital, Weill Cornell Medical College, Houston, Texas. [9]Institute for Regenerative Medicine, Wake Forest University, Winston-Salem, North Carolina. [10]Center for RNA Interference and Non-coding RNA, The University of Texas M.D. Anderson Cancer Center, Houston, Texas. [11]Department of Medicine, Division of Oncology Hematology-Oncology, University of California, Los Angeles, California. [12]Department of Psychological and Brain Sciences, University of Iowa, Iowa City, Iowa. [13]Department of Obstetrics and Gynecology, University of Iowa, Iowa City, Iowa. [14]Holden Comprehensive Cancer Center, University of Iowa, Iowa City, Iowa. [15]Department of Psychiatry, Perelman School of Medicine, University of Pennsylvania, Philadelphia, Pennsylvania. [16]Department of Cancer Biology, The University of Texas M.D. Anderson Cancer Center, Houston, Texas.

Note: Supplementary data for this article are available at Cancer Research Online (http://cancerres.aacrjournals.org/).

J.K. Allen, G.N. Armaiz-Pena, and A.S. Nagaraja contributed equally to this article.

Current address for G.N. Armaiz-Pena: Department of Basic Sciences, Division of Pharmacology, Ponce Health Sciences University and Division of Cancer Biology, Ponce Research Institute, Ponce, Puerto Rico.

Corresponding Author: Anil K. Sood, University of Texas M.D. Anderson Cancer Center, 1515 Holcombe Blvd, Unit 1362, Houston, TX 77030. Phone: 713-745-5266; Fax: 713-792-7586; E-mail: asood@mdanderson.org

doi: 10.1158/0008-5472.CAN-16-1701

Published OnlineFirst April 16, 2018; DOI: 10.1158/0008-5472.CAN-16-1701

delivery into the tumor. We found that sustained adrenergic activation leads to increased tumor growth by promoting innervation of tumors through ADRB3/cAMP/Epac-dependent induction of brain-derived neurotrophic factor (BDNF). This mechanism represents a positive feedback system that collectively functions to promote tumor growth and metastasis.

Materials and Methods

Cell lines

SKOV3ip1 and HeyA8 ovarian cancer cells were maintained as previously described (4). Colon cancer cell line RKO was a gift from Dr. Lee Ellis (Department of Surgical Oncology at The University of Texas MD Anderson Cancer Center, Houston, TX); cells were maintained in MEM media supplemented with 10% FBS and 0.1% gentamycin sulfate. $ID8^{VEGF}$ cells were a kind gift from Dr. George Coukos (Ludwig Institute for Cancer Research, Lausanne, Switzerland). These were maintained in RPMI1640 supplemented with 15% FBS, insulin–transferrin–selenium and 0.1% gentamycin. All cell lines were passaged, at most, 15 times between freeze–thaw cycles and routinely screened for *Mycoplasma* using MycoAlert Mycoplasma Detection Kit (Lonza). Authentication of cell lines was done by the Characterized Cell Line Core Facility at The University of Texas MD Anderson Cancer Center by the STR Method.

Restraint stress model

Experiments involving human and murine cell lines were performed in 8- to 12-week-old female athymic nude or C57BL/6 mice, respectively, provided by Taconic Farms. Adrenalectomized mice were acquired from Taconic Farms 3 days after surgery and given an additional 10 days to recover before restraint stress started. The University of Texas MD Anderson Cancer Center Department of Experimental Radiation Oncology provided age-matched C57/B6 mice with sham-surgeries for controls. The Institutional Animal Care and Use Committee at The University of Texas MD Anderson Cancer Center approved all animal experiments. We induced stress experimentally by using a restraint stress procedure that has been previously described (7). Tumor cells were injected intraperitoneally into mice in all groups 1 week after the stress procedure began. Ten mice were assigned to each group, and 5 days after tumor cell injection, treatment with siRNA was started (control or treatment, biweekly, 3.5 μg siRNA in DOPC or chitosan nanoparticles). The animals were sacrificed using cervical dislocation after 28 to 35 days, and mouse weight, tumor weight, number of tumor nodules, and distribution of metastases were noted.

siRNA preparation and treatment

Sequence-specific siRNA for h*BDNF*, h*NT3*, h*Artemin*, h*NGF*, *hTrkB*, *mTrkB*, and nontargeting control were obtained from Sigma-Aldrich. For *in vitro* studies, Lipofectamine 2000 transfection reagent (Invitrogen) was used according to manufacturer protocol to transiently transfect cells. For *in vivo* studies, siRNA was incorporated into DOPC neutral nanoliposomes or chitosan nanoparticles and administered as previously described (10–12).

Quantitative PCR

Total RNA was extracted from cells using the RNAeasy Mini Kit (Qiagen) and tissue RNA was extracted using TRIzol reagent (Invitrogen), according to standard manufacturer protocols. Complementary DNA was synthesized from 1 μg of total RNA using the Verso cDNA Synthesis Kit (Thermo Scientific) according to the supplier protocol, using random hexamers and oligo-dT primers in a 3:1 ratio. Quantitative PCR was performed using SYBR green and Taqman qPCR mixes on 7500 Real-Time PCR System (Applied Biosystems) using standard protocols.

Immunohistochemistry

Both frozen and paraffin-embedded sections were used for IHC. Paraffin-embedded sections of human ovarian cancer were deparaffinized in xylene and dehydrated-rehydrated in alcohol and PBS. Antigen retrieval was performed using citrate buffer in the microwave for 10 minutes. Frozen sections were fixed in acetone and acetone–chloroform. After endogenous peroxidase blocking and three washes with PBS, the slides were incubated with tyrosine hydroxylase (TH) antibody (MAB318, 1:50; Millipore), BDNF (ab72439, 1:100; Abcam), or neurofilament antibody (ab9035, 1:100, Abcam) overnight at 4°C. Matching secondary antibodies were used for 1 hour at room temperature and staining was developed using DAB. Hematoxylin was used to stain nuclei. Nerves within tumors were quantified based on presence of both individual nerves and bundles that stained positive for neurofilament or TH.

Norepinephrine concentration

Tumor catecholamine concentrations were measured using high-performance liquid chromatography as previously described (2). In brief, freshly isolated 20- to 30-mg tumor samples were frozen immediately at −80°C until extraction. The tissue was homogenized in perchloric acid, neutralized, and adsorbed onto alumina. Catecholamines were eluted and quantified by electrochemical detection. Peak chromatograph values were compared with injections of pure standards of norepinephrine. Data were reported as pg/mg or pmol/mL. Mouse catecholamine concentrations were determined by CA ELISA Kit using procedures recommended by the manufacturer (MyBioSource).

PCR neurotrophic factor array

HeyA8 cells were treated with 10 μmol/L norepinephrine for 24 hours and total RNA was extracted using RNeasy column (Qiagen). Gene expression array analysis was performed using a commercially available RT^2 Profiler PCR Array Human Neurotrophin and Receptors array (PAHS-031E-4) from SABiosciences (Qiagen), according to the manufacturer's guidelines.

BDNF promoter analysis

HeyA8 cells (3×10^5) were transfected (Lipofectamine 2000; Invitrogen) with a 1022-base pair sequence of the human *BDNF* promoter (SwitchGear Genomics) and subsequently assayed for luciferase reporter gene expression (Promega) after 3 hours of exposure to vehicle control, 10 μmol/L norepinephrine, or norepinephrine following 5-minute pretreatment with pharmacologic antagonists of β_3-adrenergic receptors or Jun N-terminal kinase (JNK). Potential Jun-responsive promoter elements were identified by TRANSFAC bioinformatic analysis of the *BDNF*-1022 sequence using the V$AP1_Q4 weight matrix (Mat_Sim score > 0.80), and the functional significance of the two putative Jun (AP1) response elements identified at −187 and −225 base pairs was evaluated by site-directed mutagenesis (T > G) to disrupt AP1 binding (13). Results represent the average fold-induction

Published OnlineFirst April 16, 2018; DOI: 10.1158/0008-5472.CAN-16-1701

across at least three independent experiments, each of which involved triplicate assays of each experimental condition.

Plasmid and transfections

Plasmid to overexpress *BDNF* was obtained from Origene. SKOV3ip1 cells were stably transfected with a virus containing control and *BDNF* plasmids and selected using puromycin. The cells were grown after selection in RPMI1640 and propagated.

Patient samples

This study was conducted following the U.S. Common Rule, with approval (including a waiver of informed consent) from the Institutional Review Boards of the MD Anderson Cancer Center and the University of Iowa Hospital and Clinics. A subset of participants completed the Center for Epidemiologic Studies Depression Scale between their preoperative appointment and surgery. This 20-item survey assesses depressive symptoms and is commonly used in studies of patients with cancer (2). Scores of 16 or higher are associated with clinical depression.

Formalin-fixed, paraffin-embedded human samples were stained for BDNF and TH. Slides were heated overnight at 65°C, followed by deparaffinization and hydration of tissue. Antigen retrieval was performed using citrate buffer (pH 6.0) for 10 minutes in the microwave, followed by cooling for 1 to 2 hours. Endogenous peroxidase activity was blocked using 3% hydrogen peroxide (in methanol) for 12 minutes. Primary antibodies were applied at a dilution of 1:100 and incubated overnight in a humidity chamber at 4°C. Horseradish peroxidase-conjugated secondary antibodies (Jackson Immunoresearch) and 3,3′-diaminobenzidine were used to visualize staining under a bright field microscope (~7–9 minutes). Counterstaining was performed using Gill's Hematoxylin for 10 seconds, followed by washing with PBS. Slides were dried and mounted using Permount. For BDNF, expression was determined by assessing semiquantitatively the percentage of stained tumor cells and the staining intensity, as described previously (14). Nerves within tumors were quantified based on presence of both individual nerves and bundles that stained positive for neurofilament or TH. An ovarian cancer tissue lacking the primary antibody was used as a negative control.

Results

Innervation of the tumor microenvironment

To test the biological significance of sustained adrenergic signaling on ovarian cancer, we first evaluated the expression of β-adrenergic receptors (ADRB) in a panel of ovarian cancer cells (Supplementary Fig. S1A). From this panel, we selected ADRB positive HeyA8, SKOV3ip1, and OVCA432 cells to study the effects of restraint stress on tumor growth and innervation. To induce tumoral catecholamine levels, we used a well-characterized restraint stress model (4, 6, 7). Restraint stress led to increased tumor growth, nodules and enhanced pattern of spread in both models and the OVCA432 model (Supplementary Fig. S1B–S1E). In the SKOV3ip1 model, daily restraint stress resulted in a significant increase ($P = 0.002$) in intratumoral nerve counts, as measured by neurofilament-L expression (Fig. 1A and B). Similar results were found in the HeyA8 model, but not in the ADRB-null A2780 model ($P = 0.02$; Fig. 1B; Supplementary Fig. S1F and S1G). In the SKOV3ip1 model, tumor samples from restraint stress animals had significantly increased intratumoral norepinephrine levels compared with controls (Fig. 1C; 3.03-fold change; $P = 0.03$; Supplementary Fig. S1H) and these were positively correlated with nerve counts (Fig. 1C; $R = 0.68$; $P = 0.01$). A similar significant increase in tumor growth, metastatic spread, and innervation in response to daily restraint stress were also found when ovarian cancer cells were surgically implanted at the primary site (i.e., ovary; Supplementary Fig. S1I–S1M).

To characterize intratumoral nerves, we performed immunohistochemical analyses for other nerve markers. We found nerves that were positive for β3-tubulin, PGP9.5 and peripherin, choline acetyltransferase and tyrosine hydroxylase (Supplementary Fig. S2A and S2B). In addition, we observed the presence of TrkB, pTrkB, and tyrosine hydroxylase positive nerves and absence of GFAP5 (Supplementary Fig. S2C and S2D). To determine if a population of intratumoral nerves were covered with myelin, we analyzed tumor samples by coherent anti-stokes Raman scattering (CARS) imaging. Our data show the presence of myelin-covered nerves (Supplementary Fig. S2E and Supplementary Movie S1–S2). Together, these data are suggestive of a heterogeneous population of intratumoral nerves that includes TH-positive nerves.

Catecholamines can be delivered locally by sympathetic nerve endings or by systemic release from the adrenal gland. Therefore, we examined the role of nerve endings as a source of catecholamine release into the tumor. Mice inoculated with SKOV3ip1 cells were subjected to daily restraint stress and treated with hexamethonium bromide, a quaternary ammonium compound that blocks ganglionic transmission by antagonizing neuronal nicotinic acetylcholine receptors in the peripheral nervous system. As expected, restraint stress significantly induced tumor growth by 5.5-fold, whereas hexamethonium bromide completely abrogated this effect (Fig. 1D; Supplementary Fig. S2F). Tumor samples from animals exposed to daily restraint stress had significantly more innervation and cAMP accumulation than tumor samples from control animals (Fig. 1E; 2.52-fold change; $P < 0.01$; Supplementary Fig. S2G); this increase was completely blocked by hexamethonium bromide (Fig. 1E). Daily restraint stress increased norepinephrine blood and tumor levels, but hexamethonium bromide did not block this effect, suggesting that the contribution of blood-delivered norepinephrine is minimal (Supplementary Fig. S2H). Moreover, hexamethonium bromide treatment resulted in a significant decrease in infiltration of F4/80+ macrophages (Supplementary Fig. S2I). To further confirm the role of sympathetic nerve endings in catecholamine-mediated tumor growth, we treated tumor bearing animals with cytisine, a nicotinic acetylcholine agonist that does not cross the brain-blood barrier. Our data show that cytisine administration leads to increased tumor growth ($P = 0.058$) and mimics the effects of restraint stress on F4/80+ macrophage infiltration (Supplementary Fig. S2J and S2K). To test the role of adrenal glands as a source of tumoral norepinephrine, we inoculated adrenalectomized mice with ID8-VEGF ovarian cancer cells and subjected them to daily restraint stress. Adrenalectomy had no significant effect on restraint stress induced tumor growth, nerve counts, and blood norepinephrine, whereas increases in tumor norepinephrine were abrogated (Fig. 1F and G; Supplementary Fig. S2L–S2M).

Norepinephrine induces BDNF expression through an ADRB3/cAMP/Epac/Jnk signaling axis

To elucidate the mechanism used by tumor cells to induce nerve growth, we analyzed microarray data obtained from HeyA8 and SKOV3ip1 cells exposed to norepinephrine for 3 hours to identify functional networks that play a role in

Published OnlineFirst April 16, 2018; DOI: 10.1158/0008-5472.CAN-16-1701

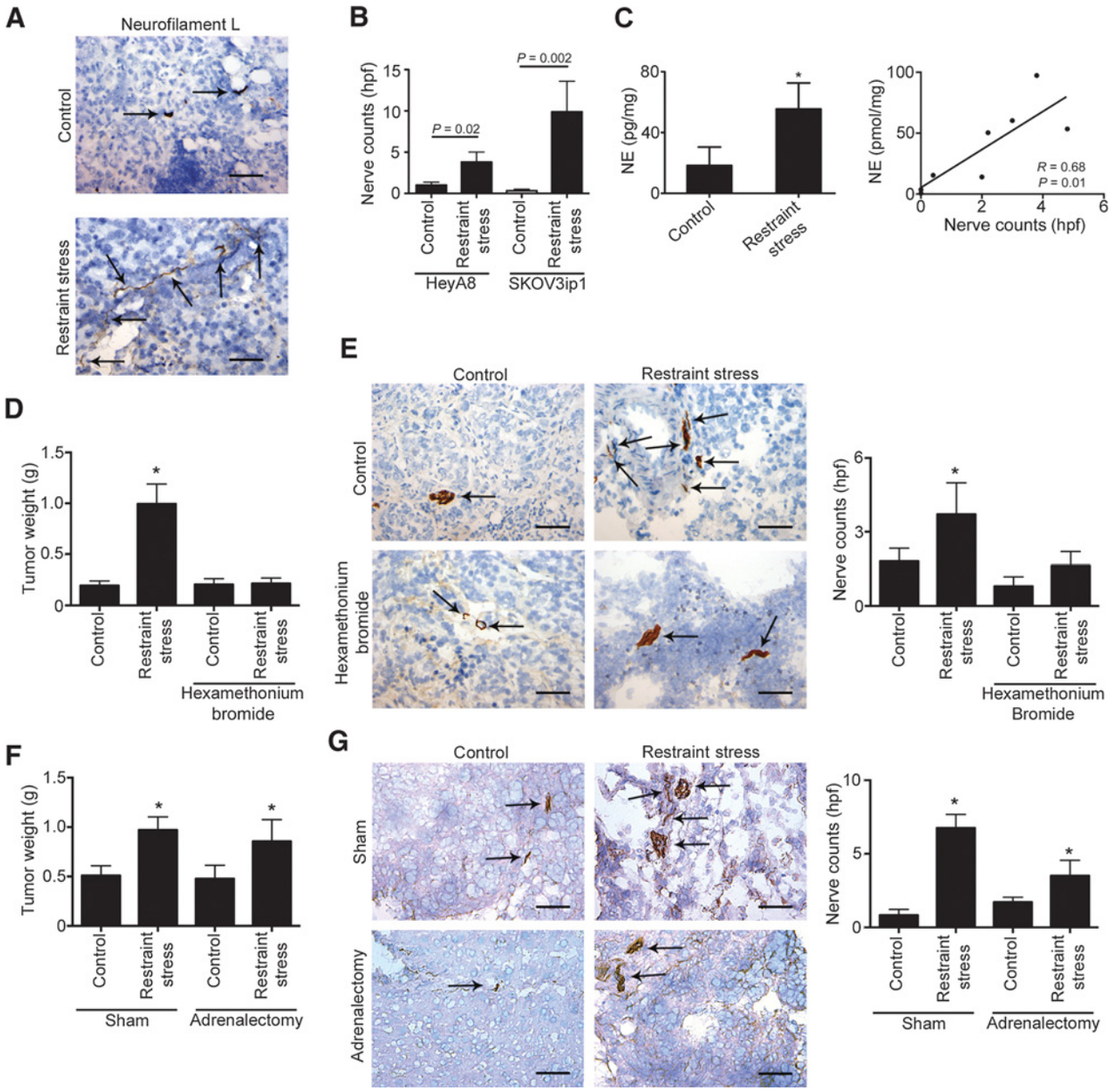

Figure 1.

Sustained adrenergic signaling increases nerve counts in tumors. **A,** Neurofilament expression in orthotopic SKOV3ip1 tumors in control and mice exposed to restraint stress. **B,** Nerve counts in orthotopic SKOV3ip1 and HeyA8 tumors. **C,** Norepinephrine (NE) levels in SKOV3ip1 tumors and correlation with nerve counts within the tumors. **D** and **E,** Tumor growth (**D**) and nerve counts (**E**) in SKOV3ip1 tumors exposed to hexamethonium bromide and restraint stress. **F** and **G,** Tumor growth (**F**) and nerve counts (**G**) in sham and adrenalectomized mice exposed to restraint stress. Results represent the mean ± SEM; $n = 10$ mice per group. *, $P < 0.05$. Scale bar, 50 μm.

neuronal growth and function. To perform these analyses, we employed Affymetrix U133A high-density oligonucleotide arrays (data deposited at NCBI GEO as GSE34405; ref. 4). Data collected from this approach was subjected to pathway enrichment analyses using NetWalker (15). Top interacting networks that were most differentially expressed between untreated and norepinephrine-treated cells. Common networks identified in both cell lines are shown in Fig. 2A. These analyses revealed that networks related to neuronal growth and functions were among the most significantly upregulated pathways following norepinephrine treatment in both cell lines (Supplementary Table S1). Six genes were identified to be common contributors of these pathways (Fig. 2A). Out of these genes, we focused on BDNF and its role in tumor cell-induced neuronal growth because it was upregulated in both cell lines by more than 2.5-fold (Fig. 2A). To validate these findings, we treated SKOV3ip1 cells with norepinephrine and analyzed changes in 84 known neurotrophic factors. This analysis identified BDNF as

Published OnlineFirst April 16, 2018; DOI: 10.1158/0008-5472.CAN-16-1701

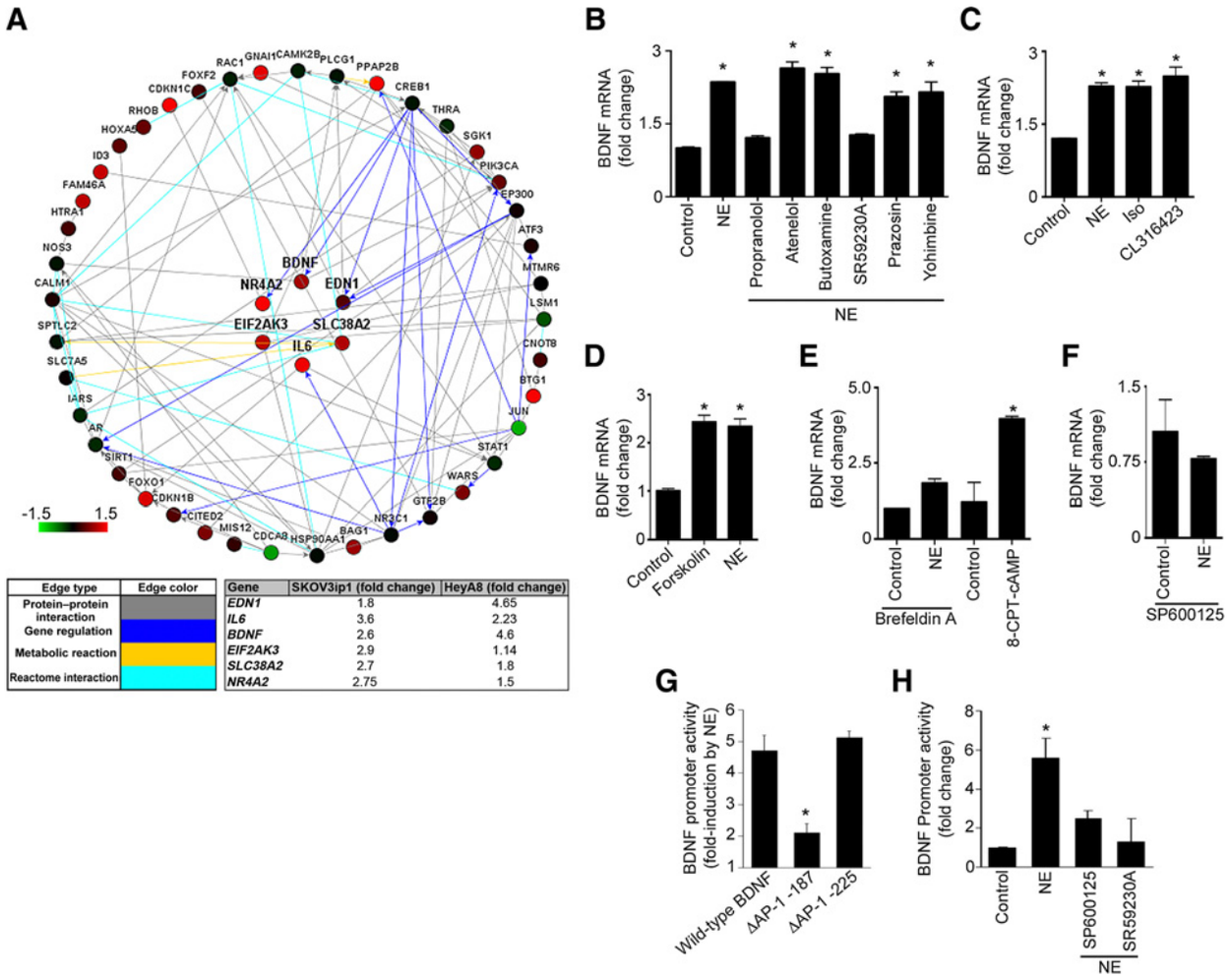

Figure 2.

Norepinephrine induced BDNF expression. **A,** Network map of upregulated genes involved in neuronal growth and function. **B,** Relative expression levels of BDNF in norepinephrine (NE)-treated cells with nonspecific and specific ADRB blockers. **C,** After treatment with norepinephrine, Iso, or ADRB3-specific agonist. **D,** After treatment with forskolin. **E,** After treatment with Brefeldin A (Epac antagonist) or 8CPT-2Me-cAMP (Epac agonist). **F,** After treatment with SP600125 (Jnk antagonist) and norepinephrine. BDNF promoter activity after treatment with norepinephrine (**G**) or norepinephrine and SP600125 (Jnk antagonist) or norepinephrine and SR59230A (ADRB3 blocker; **H**). *, $P < 0.05$.

one of the most upregulated genes after norepinephrine treatment (Supplementary Fig. S3A). Quantitative RT-PCR analyses of several of these factors confirmed that BDNF is significantly upregulated after norepinephrine treatment (Supplementary Fig. S3B). Next, we compared BDNF expression in a panel that included normal ovarian epithelial cells and ovarian cancer cell lines. Ovarian cancer cells have significantly higher levels of BDNF when compared with normal ovarian epithelial cells (Supplementary Fig. S3C). Furthermore, to extend these data to our *in vivo* models, we analyzed samples from tumor-bearing mice that were subjected to 1, 2, or 3 weeks of daily restraint stress and determined tumoral BDNF levels by qRT-PCR. BDNF levels were significantly increased in a time-dependent manner (Supplementary Fig. S3D). Next, we confirmed the efficacy of siRNA for silencing BDNF levels in SKOV3ip1 cells as these will be used throughout the experiments presented here (Supplementary Fig. S3E and S3F).

Next, we examined the potential underlying mechanisms by which catecholamines induce BDNF levels. Given that norepinephrine can affect α- and β-adrenergic receptors, we first tested the individual contribution of each receptor to norepinephrine-induced BDNF expression. Norepinephrine treatment significantly increased BDNF gene and protein levels (Fig. 2B; Supplementary Fig. S4A; $P < 0.05$) in ovarian cancer cells. Next, we validated specific adrenergic agonists and antagonists by measuring intracellular cAMP levels in response to them (Supplementary Fig. S4B). Exposure to specific blockers followed by norepinephrine demonstrated that only inhibition of ADRB3 abrogated norepinephrine-induced BDNF gene or protein expression (Fig. 2A; Supplementary Fig. S4C and S4D). Conversely, the use of an ADRB3 agonist induced BDNF gene and protein expression ($P < 0.05$; Fig. 2C; Supplementary Fig. S4E).

Next, we examined the downstream signaling activated in response to norepinephrine. Forskolin, a cAMP agonist,

Published OnlineFirst April 16, 2018; DOI: 10.1158/0008-5472.CAN-16-1701

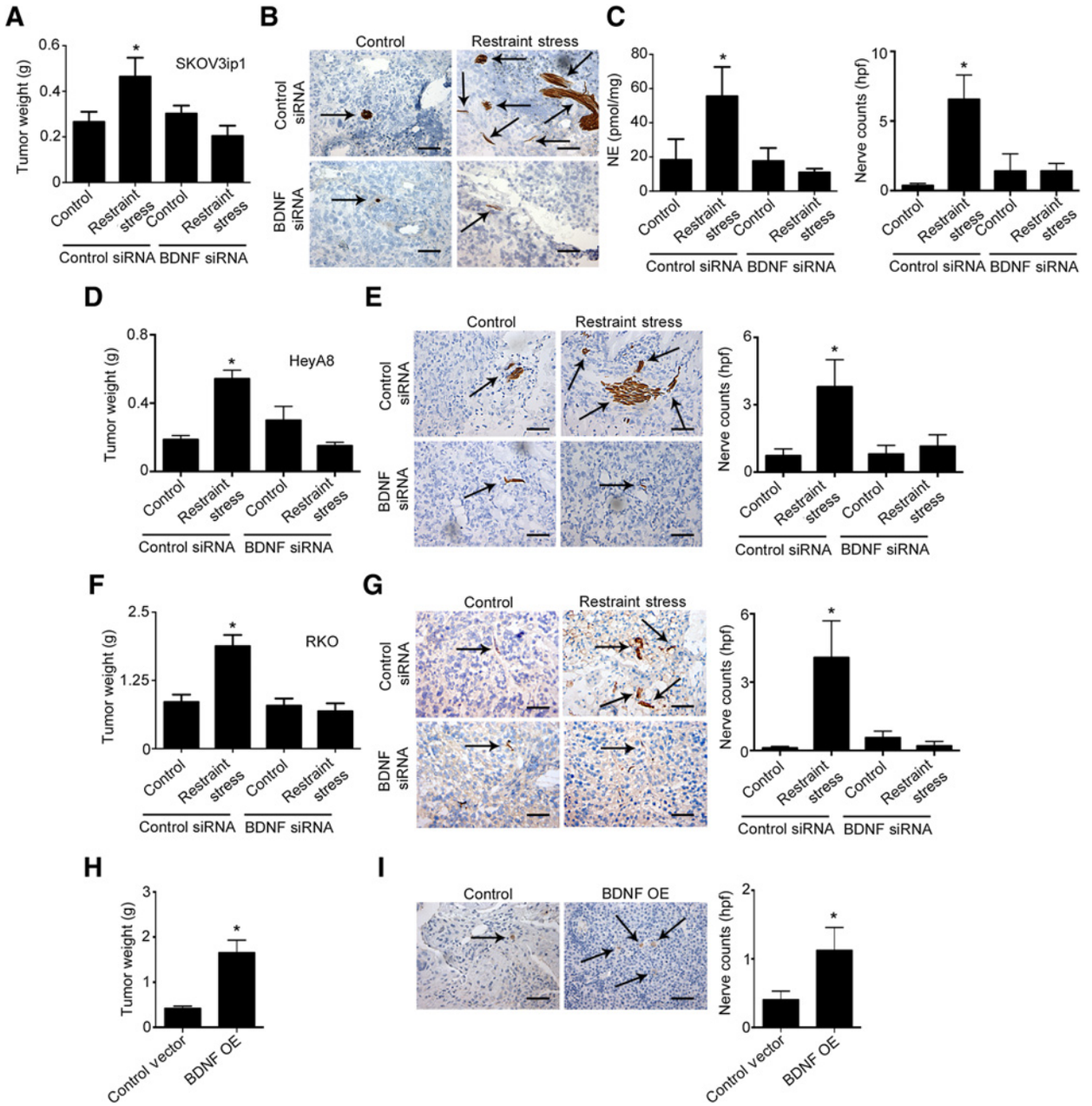

Figure 3.

Increased nerve counts are driven by BDNF induction. **A,** Tumor weight in restraint stress orthotropic mouse model with control or BDNF siRNA-DOPC. **B,** Nerve counts of tumors in each group in the SKOV3ip1 model. **C,** Intratumoral norepinephrine (NE) levels in each group in the SKOV3ip1 model. **D,** Tumor weight in restraint stress orthotopic models treated with control or BDNF-DOPC siRNA. **E,** Nerve counts of tumors in each group in the HeyA8 model. **F,** Tumor weight in restraint stress orthotopic RKO colon cancer model. **G,** Nerve counts of tumors in each group in the RKO model. **H,** Tumor weight in control and BDNF overexpressing SKOV3ip1 model. **I,** Nerve counts of tumors in each group. Means and SE of the mean are shown. $N = 10$ mice per group.
*, $P < 0.05$. Scale bar, 50 μm.

significantly increased BDNF gene and protein production (Fig. 2D; Supplementary Fig. S4D; $P < 0.01$). Given that cAMP increases can be associated with parallel PKA, PKC, or Epac activity, we investigated their potential role in adrenergic mediated BDNF induction. PKA or PKC inhibitors failed to abrogate norepinephrine-induced BDNF expression (Supplementary Fig. S4F). The Epac inhibitors, Brefeldin A and ESI-05, significantly abrogated norepinephrine-induced BDNF expression, whereas 8CPT-2Me-cAMP (Epac activator) significantly increased BDNF expression (Fig. 2E; $P < 0.01$; Supplementary Fig. S4G). To elucidate potential downstream signaling events mediated by the ADRB3/Epac signaling axis, we used JNK, MEK, PLC, PI3K, MAPK, and PKA

Published OnlineFirst April 16, 2018; DOI: 10.1158/0008-5472.CAN-16-1701

inhibitors and studied their effect on norepinephrine-induced BDNF expression. JNK was found to be the key downstream mediator of norepinephrine induced BDNF gene and protein induction (Fig. 2F; Supplementary Fig. S4H–S4J). JNK exerts this control through the regulation of AP-1. To understand how BDNF gene expression is regulated by AP-1, we performed promoter luciferase assays. Norepinephrine increased BDNF promoter activity, and this induction was blocked by mutation of the AP-1 binding site 187 bp upstream of the BDNF transcription start site (but not the AP-1 site 225 bp upstream), and blocked by an ADRB3 blocker and by a JNK inhibitor (Fig. 2G and H; Supplementary Fig. S4H–S4J).

Sustained adrenergic signaling requires tumor-derived BDNF to promote innervation

We next investigated the role of BDNF in the promotion of tumor innervation in response to sustained adrenergic signaling. Mice inoculated with SKOV3ip1 or HeyA8 cells were subjected to daily restraint stress and treated with either control siRNA-DOPC or BDNF siRNA-DOPC. In both models, restraint stress resulted in increased tumor growth, whereas BDNF siRNA-DOPC completely abrogated this effect (Fig. 3A–E; Supplementary Fig. S5A and S5B). A second BDNF siRNA sequence had the same effect seen in the previous experiment (Supplementary Fig. S5C and S5D). The increase in tumor growth in response to daily restraint stress was also accompanied by increased nerve counts and tumoral norepinephrine levels, but both of these effects were blocked by BDNF siRNA-DOPC (Fig. 3A–E). Moreover, BDNF gene and protein levels were significantly elevated after restraint stress and significantly reduced after treatment with BDNF-siRNA-DOPC (Supplementary Fig. S5E and S5F). To determine whether similar findings would be noted in other types of cancer, we used a well-characterized colon cancer model. For this model, RKO cells were selected due to their sensitivity to ADRB signaling, as measured by increased BDNF gene levels upon norepinephrine treatment (Supplementary Fig. S5G). In tumors derived from the RKO colon cancer cell line, we found significant increases in tumor weight and nerve counts following daily restraint stress and these effects were abrogated by treatment with BDNF siRNA-DOPC (Fig. 3F and G). We then generated stable SKOV3ip1 clones that overexpress BDNF to assess whether increased BDNF levels were sufficient to stimulate tumor innervation and tumor growth. After confirming BDNF overexpression (Supplementary Fig. S5H), we inoculated mice with either BDNF overexpressing cells (BDNF OE) or control vector SKOV3ip1 cells. After four weeks, mice were sacrificed and tumor growth and innervation were examined. BDNF OE resulted in significantly increased tumor growth and nerve counts when compared with the control group (Fig. 3H and I).

We next considered whether increased BDNF levels could drive tumor growth by signaling through tumor cell or nerve TrkB receptors. To study the contribution of these independent pathways, we subjected SKOV3ip1 tumor bearing mice to daily restraint stress and either control siRNA-DOPC or a validated human TrkB siRNA-DOPC (Supplementary Fig. S6A and S6B). Human TrkB siRNA (targeting cancer cell line) did not block stress-induced tumor growth and increased innervation (Fig. 4A and B; Supplementary Fig. S6C). Conversely, use of a validated murine TrkB siRNA delivered in a chitosan nanoparticle entirely abrogated restraint stress–induced tumor growth and innervation (Fig. 4C and D; Supplementary Fig. S6D–S6F). To further validate these results, we utilized a TrkB Kinase-Switch mouse model (16), which allows for inducible, reversible inhibition of TrkB receptors when 1NaPP1 is administered. These mice were inoculated with ID8-VEGF and subjected to daily restraint stress and treated with daily vehicle or 1NaPP1. Restraint stress induced tumor growth and innervation in vehicle treated groups, whereas TrkB inhibition completely blocked restraint stress induced tumor growth and innervation (Fig. 4E and F; Supplementary Fig. S6G). These data suggest that adrenergic-induced tumoral BDNF production leads to a feed-forward loop in which tumor growth is increased by the promotion of nerve growth.

High BDNF expression and tumor nerve counts are associated with poor outcome in patients with ovarian cancer

We first characterized the degree of BDNF protein expression and nerve counts in tumors from a cohort of patients with ovarian cancer ($n = 108$) and examined if there was an association with survival and clinicopathologic variables. Eighty-eight percent of the examined patients had tumors with serous histology and 87% had high-grade carcinomas. Eighty-three percent of patients had advanced stage disease at initial diagnosis and 74% had associated ascites. Of the tumor specimens evaluated, 47% had high BDNF expression and 53% had low expression (Fig. 5A; Supplementary Table S2). High BDNF was significantly associated with advanced tumor stage, presence of ascites, suboptimal cytoreduction, and increased mortality in these patients (Fig. 5A; Supplementary Table S2). We also determined the extent of innervation in this cohort. High nerve counts were significantly associated with advanced stage, presence of ascites and decreased survival (Fig. 5B; Supplementary Table S3). To determine whether nerve counts were independently associated with patient survival, a multivariable analysis was performed that controlled for patient age, tumor stage, histology, and degree of cytoreduction. Similar to the results above, increased nerve counts remained statistically significantly associated with patient survival ($P < 0.001$). Furthermore, in a subset of samples, we found a positive correlation between BDNF, nerve counts, and intratumoral norepinephrine (Fig. 5C and D; $R = 0.77$; $P < 0.001$).

Discussion

Here, we report a feed-forward loop that provides the underlying mechanism by which sustained adrenergic signaling can increase tumor innervation, resulting in increased norepinephrine accumulation and enhanced tumor growth. Other studies have reported that prostate tumors are infiltrated by autonomic nerve projections (9), but the underlying mechanisms were not fully understood. It is likely that tumoral innervation is a key component of the tumor microenvironment that fuels cancer progression since the newly developed nerve endings can release growth promoting catecholamines. The presence of neurotrophic factors and neuronal markers in the tumor microenvironment has been correlated with worse prognosis among patients with cancer, but the underlying mechanisms were not well understood. Here, we report on the role of cancer cells as inducers of innervation and the biological consequences of this process. Upon adrenergic stimulation, mediated through the ADRB3 receptor, cancer cells secrete BDNF, which signals through the nerve TrkB receptor and results in increased innervation. This process is likely due to the recruitment of

Published OnlineFirst April 16, 2018; DOI: 10.1158/0008-5472.CAN-16-1701

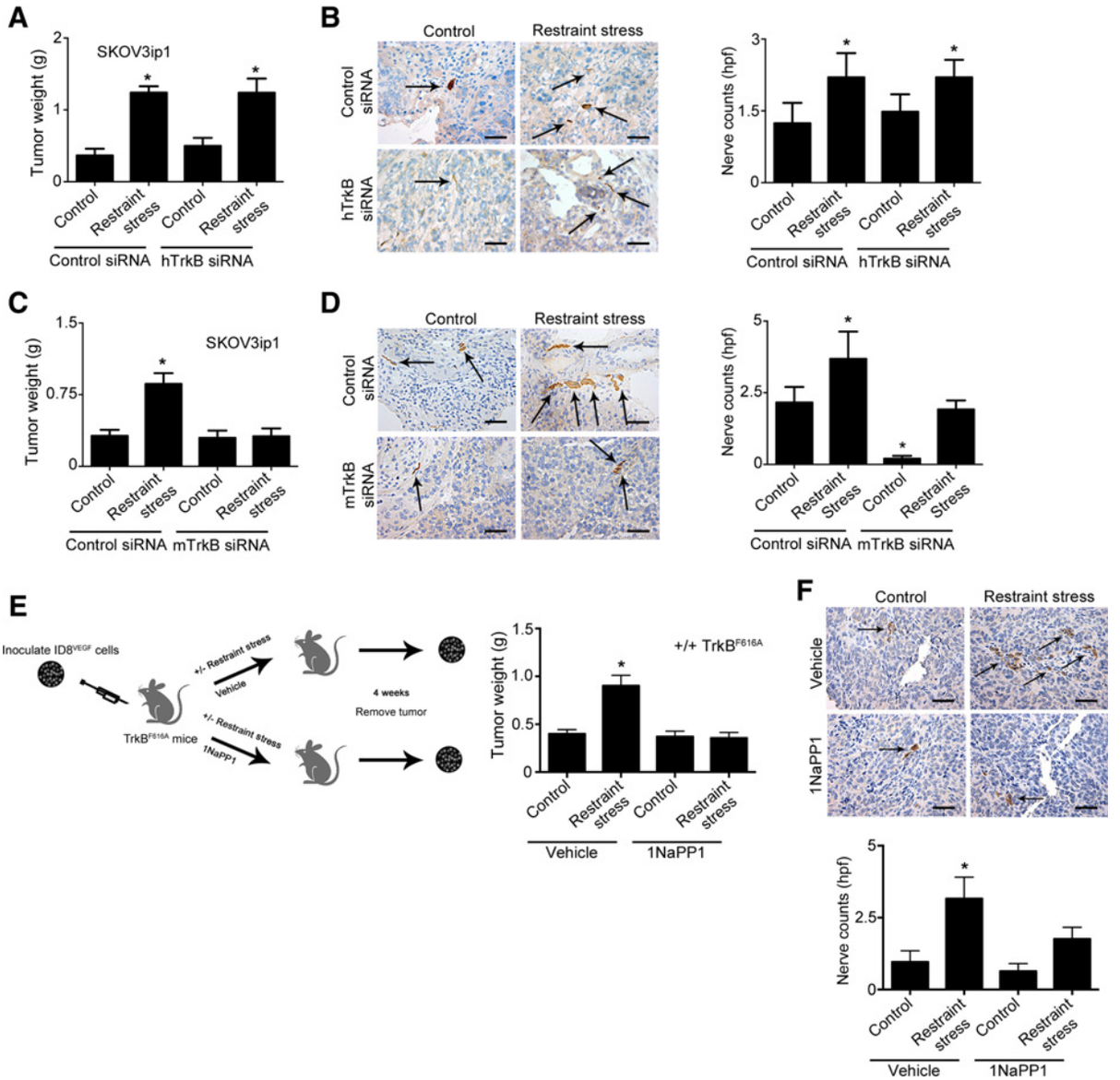

Figure 4.

Adrenergic-mediated mTrkB activation leads to increased tumor growth and nerve counts. **A,** Tumor weight in restraint stress orthotopic SKOV3ip1 models treated with control or hTrkb siRNA-DOPC. **B,** Nerve counts of tumors in each group in the hTrkb siRNA SKOV3ip1 model. **C,** Tumor weight in restraint stress orthotopic SKOV3ip1 mouse models treated with control or mTrkB siRNA-chitosan. **D,** Nerve counts of tumors in each group in the mTrkB siRNA SKOV3ip1 model. **E,** Tumor weight in restraint stress +/+TrkB^{F616A} mouse models treated with vehicle or 1NaPP1. **F,** Nerve counts of tumors in each group in the ID8-VEGF tumor-bearing +/+TrkB^{F616A} mouse model. Means and SE of the mean are shown; $n = 10$ mice per group. *, $P < 0.05$. Scale bar, 50 μm.

mesenchymal stem cells from the bone marrow and/or arborization of established nerves into the tumor microenvironment. Our results also showed that increased nerve counts are associated with higher intratumoral norepinephrine. These data provide the underlying mechanism behind how stress hormones get to the tumor microenvironment, activate ADRB-dependent pathways and result in increased angiogenesis (e.g., VEGF, IL6) and metastasis (e.g., FAK, Src, MMPs; refs. 4, 6, 7, 17, 18). Moreover, innervation of the tumor microenvironment was largely dependent on stress hormones delivered directly into the tumor by nerve endings and not from adrenal glands. Although our findings indicate that tumoral innervation is driven by the ADRB3/BDNF axis, it is possible that other factors might play a role. For example, we found that the tumor microenvironment is innervated with sensory, motor, and adrenergic nerves, suggesting nerve heterogeneity and function. Furthermore, our data show that norepinephrine stimulation results in BDNF induction that is mediated by ADRB3 and not by other adrenergic receptors. Activation of specific downstream machinery by each ADRB receptor is not surprising

Published OnlineFirst April 16, 2018; DOI: 10.1158/0008-5472.CAN-16-1701

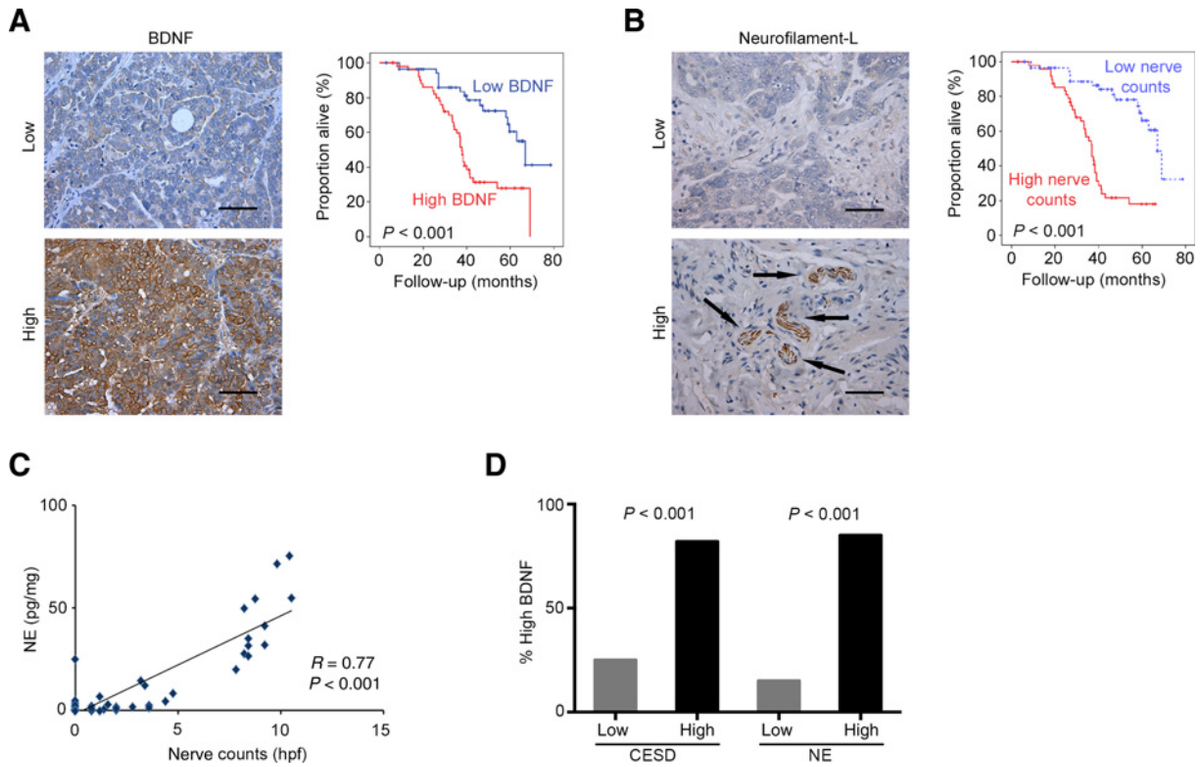

Figure 5.

High BDNF expression and tumor nerve counts correlate with poor outcome in patients with ovarian cancer. **A,** BDNF expression in human ovarian tumors and Kaplan–Meier curves of disease-specific survival in patients with epithelial ovarian carcinoma ($n = 108$) with high or low BDNF expression. **B,** Nerve counts in human ovarian tumors and Kaplan–Meier curves of disease-specific survival in patients with epithelial ovarian carcinoma ($n = 108$) with high or low nerve counts. **C** and **D,** Correlation of intratumoral norepinephrine (NE) levels in human ovarian tumor samples with nerve counts (**C**) and association of Center for Epidemiologic Studies Depression Scale (CESD) scores and intratumoral norepinephrine with BNDF (**D**). Scale bar, 50 μm.

as emerging data points toward a more complex adrenergic mediated signal transduction pathway than the classical ADRB/G-coupled subunits/AC system (19–21). Together, these data implicate tumor innervation as an important driver of tumor growth.

This work resolves key mechanisms underlying the mounting data regarding the relevance of targeting sustained adrenergic signaling in the treatment of patients with cancer. It identifies ADRB3 blockers as a potential strategy for blocking the deleterious effects of altered neuroendocrine factors and improving patient outcomes. Our work also provides a rationale for targeting the BDNF/TrkB signaling axis, which creates a hospitable tumor microenvironment when influenced by sustained adrenergic signaling. These mechanisms, by which nerves infiltrate the tumor microenvironment, rewire the host and assert ultimate sovereignty.

Disclosure of Potential Conflicts of Interest

No potential conflicts of interest were disclosed.

Authors' Contributions

Conception and design: J.K. Allen, A.S. Nagaraja, G. Lopez-Berestein, M. De Biasi, A.K. Sood

Development of methodology: J.K. Allen, N.C. Sadaoui, W. Hu, J. Bottsford-Miller, C. Rodriguez-Aguayo, F.C. Marini, A.K. Sood

Acquisition of data (provided animals, acquired and managed patients, provided facilities, etc.): J.K. Allen, G.N. Armaiz-Pena, A.S. Nagaraja, N.C. Sadaoui, T. Ortiz, R. Dood, D.M. Herder, K.M. Gharpure, R. Rupaimoole, R.A. Previs, S. Pradeep, X. Xu, H. Dong Han, B. Zand, H.J. Dalton, M. Taylor, W. Hu, J. Bottsford-Miller, M. Moreno-Smith, Y. Kang, E.L. Spaeth, S.T.C. Wong, F.C. Marini, S.W. Cole, A.K. Sood

Analysis and interpretation of data (e.g., statistical analysis, biostatistics, computational analysis): G.N. Armaiz-Pena, A.S. Nagaraja, M. Ozcan, M. Haemmerle, R. Rupaimoole, S.Y. Wu, H.J. Dalton, M. Taylor, W. Hu, V. Sehgal, P.T. Ram, S.T.C. Wong, G. Lopez-Berestein, S.W. Cole, M. De Biasi, A.K. Sood

Writing, review, and/or revision of the manuscript: G.N. Armaiz-Pena, A.S. Nagaraja, N.C. Sadaoui, M. Ozcan, R.A. Previs, S.Y. Wu, B. Zand, L.S. Mangala, P.T. Ram, G. Lopez-Berestein, S.W. Cole, S.K. Lutgendorf, M. De Biasi, A.K. Sood

Administrative, technical, or material support (i.e., reporting or organizing data, constructing databases): J.K. Allen, N.C. Sadaoui, R. Dood, M. Ozcan, M. Taylor, W. Hu, A.K. Sood

Study supervision: A.K. Sood

Acknowledgments

G.N. Armaiz-Pena was partially supported by an institutional development award from the NIGMS P20GM103475, a grant from the Puerto Rico Science, Technology and Research Trust, and the following grants NCI U54CA163071, U54CA163068, and G12MD007579. A.S. Nagaraja was supported, in part, by the CPRIT Graduate Scholar Fellowship (RP140106). B. Zand, H.J. Dalton, R.A. Previs, and J. Bottsford-Miller were supported by an NIH T32 Training Grant CA101642. S.K. Lutgendorf was supported by NIH grants CA140933 and CA193249. S.Y. Wu was supported by Ovarian Cancer Research Fund, Inc. and

Published OnlineFirst April 16, 2018; DOI: 10.1158/0008-5472.CAN-16-1701

Cancer Prevention Research Institute of Texas training grants (RP101502 and RP101489). M. De Biasi was supported by NIH grant U19CA148127, Area 2. This work was also supported in part by NIH grants (CA109298, P50 CA217685, R35 CA209904, P50CA098258, CA016672, U54CA96300, and U54CA96297), Ovarian Cancer Research Fund Program Project Development Grant, the Frank McGraw Memorial Chair in Cancer Research, the American Cancer Society Research Professor Award, and the Blanton-Davis Ovarian Cancer Research Program to A.K. Sood.

The costs of publication of this article were defrayed in part by the payment of page charges. This article must therefore be hereby marked *advertisement* in accordance with 18 U.S.C. Section 1734 solely to indicate this fact.

Received June 28, 2016; revised April 4, 2017; accepted April 10, 2018; published first April 16, 2018.

References

1. Cole SW, Arevalo JM, Takahashi R, Sloan EK, Lutgendorf SK, Sood AK, et al. Computational identification of gene-social environment interaction at the human IL6 locus. Proc Natl Acad Sci U S A 2010;107:5681–6.
2. Lutgendorf SK, DeGeest K, Sung CY, Arevalo JM, Penedo F, Lucci J 3rd, et al. Depression, social support, and beta-adrenergic transcription control in human ovarian cancer. Brain Behav Immun 2009;23:176–83.
3. Hassan S, Karpova Y, Baiz D, Yancey D, Pullikuth A, Flores A, et al. Behavioral stress accelerates prostate cancer development in mice. J Clin Invest 2013;123:874–86.
4. Armaiz-Pena GN, Allen JK, Cruz A, Stone RL, Nick AM, Lin YG, et al. Src activation by beta-adrenoreceptors is a key switch for tumour metastasis. Nat Commun 2013;4:1403.
5. Shahzad MM, Arevalo JM, Armaiz-Pena GN, Lu C, Stone RL, Moreno-Smith M, et al. Stress effects on FosB- and interleukin-8 (IL8)-driven ovarian cancer growth and metastasis. J Biol Chem 2010;285:35462–70.
6. Sood AK, Armaiz-Pena GN, Halder J, Nick AM, Stone RL, Hu W, et al. Adrenergic modulation of focal adhesion kinase protects human ovarian cancer cells from anoikis. J Clin Invest 2010;120:1515–23.
7. Thaker PH, Han LY, Kamat AA, Arevalo JM, Takahashi R, Lu C, et al. Chronic stress promotes tumor growth and angiogenesis in a mouse model of ovarian carcinoma. Nat Med 2006;12:939–44.
8. Armaiz-Pena GN, Cole SW, Lutgendorf SK, Sood AK. Neuroendocrine influences on cancer progression. Brain Behav Immun 2013;30 Suppl: S19–25.
9. Magnon C, Hall SJ, Lin J, Xue X, Gerber L, Freedland SJ, et al. Autonomic nerve development contributes to prostate cancer progression. Science 2013;341:1236361.
10. Landen CN Jr, Chavez-Reyes A, Bucana C, Schmandt R, Deavers MT, Lopez-Berestein G, et al. Therapeutic EphA2 gene targeting in vivo using neutral liposomal small interfering RNA delivery. Cancer Res 2005;65: 6910–8.
11. Lu C, Han HD, Mangala LS, Ali-Fehmi R, Newton CS, Ozbun L, et al. Regulation of tumor angiogenesis by EZH2. Cancer Cell 2010;18: 185–97.
12. Stone RL, Nick AM, McNeish IA, Balkwill F, Han HD, Bottsford-Miller J, et al. Paraneoplastic thrombocytosis in ovarian cancer. N Engl J Med 2012;366:610–8.
13. Angel P, Imagawa M, Chiu R, Stein B, Imbra RJ, Rahmsdorf HJ, et al. Phorbol ester-inducible genes contain a common cis element recognized by a TPA-modulated trans-acting factor. Cell 1987;49:729–39.
14. Sood AK, Coffin JE, Schneider GB, Fletcher MS, DeYoung BR, Gruman LM, et al. Biological significance of focal adhesion kinase in ovarian cancer: role in migration and invasion. Am J Pathol 2004;165:1087–95.
15. Komurov K, Dursun S, Erdin S, Ram PT. NetWalker: a contextual network analysis tool for functional genomics. BMC Genomics 2012;13:282.
16. Chen X, Ye H, Kuruvilla R, Ramanan N, Scangos KW, Zhang C, et al. A chemical-genetic approach to studying neurotrophin signaling. Neuron 2005;46:13–21.
17. Sood AK, Bhatty R, Kamat AA, Landen CN, Han L, Thaker PH, et al. Stress hormone-mediated invasion of ovarian cancer cells. Clin Cancer Res 2006;12:369–75.
18. Nilsson MB, Armaiz-Pena G, Takahashi R, Lin YG, Trevino J, Li Y, et al. Stress hormones regulate interleukin-6 expression by human ovarian carcinoma cells through a Src-dependent mechanism. J Biol Chem 2007; 282:29919–26.
19. Hur EM, Kim KT. G protein-coupled receptor signalling and cross-talk: achieving rapidity and specificity. Cell Signal 2002;14:397–405.
20. Lefkowitz RJ, Pierce KL, Luttrell LM. Dancing with different partners: protein kinase a phosphorylation of seven membrane-spanning receptors regulates their G protein-coupling specificity. Mol Pharmacol 2002;62:971–4.
21. Steinberg SF. beta(2)-Adrenergic receptor signaling complexes in cardiomyocyte caveolae/lipid rafts. J Mol Cell Cardiol 2004;37:407–15.

Cancer Research
The Journal of Cancer Research (1916–1930) | The American Journal of Cancer (1931–1940)

AACR American Association for Cancer Research

Sustained Adrenergic Signaling Promotes Intratumoral Innervation through BDNF Induction

Julie K. Allen, Guillermo N. Armaiz-Pena, Archana S. Nagaraja, et al.

Cancer Res 2018;78:3233-3242. Published OnlineFirst April 16, 2018.